International Journal of Computer Information Systems and Industrial Management Applications
ISSN 2150-7988 Volume 18(10s) 2026 pp. 147-166
https://doi.org/10.70917/ijcisim-2026-3574
Article

Automated Classification of Diabetic Eye Diseases Using Optimized Deep Convolutional Model

N. Prakash[1], S.Padmalal[2], K Devipriya[3], Madhulika Yarlagadda[4], SNV Ramana Murthy Banda [5], M.Pompapathi[6]

[1]Department of IT, Sreenidhi Institute of science and technology, Hyderabad, Telangana
India-501301
prakash.nakirekanti@gmail.com
[2]Department of Computer science and Engineering, Mangalam College of Engineering,Kottayam District. Kerala,INDIA
splaal71@gmail.com
ORCID Id: https://orcid.org/ 0000-0002-4552-767X
Official id: padmalal.s@mangalam.in
[3]Department of CSE, Lakireddy Bali Reddy College of Engineering, Andhra Pradesh,INDIA
k.devipriya20@gmail.com
0000-0003-4799-6020]
[4]CSE Department, Amity School of engineering and Technology, Amity University, Hyderabad
madhulika.yarlagadda@gmail.com
0000-0002-6132-643X
[5]Department of CSE-AIML, ADITYA UNIVERSITY, SURAMPALEM,A.P.
ramanamurthy.banda@gmail.com
https://orcid.org/0009-0003-8371-1691
[6]Department of Information Technology,RVR & JC College of Engineering ,Guntur , Andhra Pradesh - 522019INDIA.
E-Mail :manasani.pompapathi@gmail.com
Orcid Id :0000-0002-4884-9754

Abstract: Diabetic retinopathy is a diabetic complication caused by damage to the blood vessels of the light-sensitive tissue at the back of the retina. This disease has no early symptoms and can lead to blindness. In recent decades, the Deep Learning (DL) approaches have provided a way to accurately detect and classify this eye disease, which helps medical professionals plan treatment procedures. In this study, a novel automatic diabetic retinopathy classification model was proposed by leveraging the efficiency of the Honey Badger Algorithm and Deep Convolutional Neural Network (HBA-DCNN). The retinal images are initially collected and then preprocessed to standardize the images effectively for subsequent processes. Consequently, the image segmentation used superpixel mean orientation to capture the Region of Interest (ROI) from the preprocessed images. Finally, the retinopathy classification was performed using the proposed HBA-DCNN model. The DCNN in the proposed framework learns the patterns differentiating normal and diabetic retinopathy by capturing the most informative and distinct features. The HBA algorithm refines the parameters of the DCNN to its optimal range, which helps reduce the computational time and improves the training performances. The presented methodology was trained and validated using the publicly available two databases, namely Digital Retinal Image for Vessel Extraction (DRIVE) and Structured Analysis of the Retina (STARE), and the experimental results are assessed in terms of accuracy, precision, recall, and F-measure. In addition, the implementation outcomes are compared and validated with state-of-the-art techniques such as Deep Neural Network (DNN) in addition to Support Vector Machine (SVM).
Keywords: Diabetic retinopathy, convolutional neural network, Gabor filtering, median filtering, honey badger algorithm, and deep learning model.

1. Introduction

Unlike the manual trial of the fundus by a trained specialist known as instant ophthalmology, computer-assisted diagnosis becomes an option for detecting retinal fundus images [1]. Besides, the computer-assisted diagnosis of retina fundus helped determine the images, proved as solid as instant ophthalmic medicine, and required less excellent chance of manipulation and breaking [2]. Various eye-related symptoms that can lead to visual impairment, such as macular degeneration and diabetic retinopathy, are continuously analyzed using retinal fundus images. One of the essential advances in detecting diabetic retinopathy is the extraction of retinal nerves from the fundus films [3]. Although some division techniques have been proposed, this section remains experimental due to variations in the retinal vasculature structure and image quality [4].

Currently, the fundamental challenges of retinal vessel segmentation are noise (often bright luminosity) and thin vessels [5]. Besides, most proposed segmentation techniques focus on individually improving each dataset's preprocessing and shipping segment boundaries. As a result, these methods can continue to achieve high accuracy for enhanced databases, although accuracy decreases whenever applied to other databases [6]. Even though ship division strategies generally have preprocessing steps to improve the ship's presence, a few steps begin with the division step, except the preprocessing steps. Nowadays, many sectoral strategies rely on Artificial Intelligence (A.I.) [7] ideas combined with conventional sectoral practices to improve the segmentation accuracy of their strategy by providing an honest inquiry into the information that aids segment calculations [8].

These machine-learning ideas can be broadly categorized as supervised and unsupervised approaches in light of the use of named information. In supervised mode, each pixel in the image is marked by a human administrator and assigned to the class [9], i.e., non-vessel and vessel. The progress of the element vectors is generated from the information being handled (pixel-wise elements in image segment issues) and categorized using the names assigned to the information. A separate system uses pre-defined highlight vectors without class names, where comparison examples are collected for specific classes [10].

Contribution and organization of the work

- This study proposes an automatic diabetic retinopathy classification strategy by leveraging deep learning and meta-heuristic optimization algorithms.
- The proposed framework uses a superpixel mean orientation approach for performing image segmentation. This approach captures the ROI from the preprocessed images and helps locate the infected region.
- The classification module was developed by integrating the features of DCNN and HBA. The DCNN model learns the patterns distinguishing normal and diabetic retinopathy instances through practical training and performs Classification.
- The HBA model optimizes and fine-tunes DCNN's hyperparameters, improving the overall classification performance.
- The proposed method is implemented in Python, and its performance is evaluated using performance metrics such as recall, precision, accuracy, sensitivity, and F-measure.

The article's enduring sections are organized as follows: Section 2 reviews existing eye disease classification and segmentation works. Section 3 presents a detailed explanation of the proposed technique. Section 4 explains the research outcomes. The final portion summarises the paper.

2. Related works

The automated prediction of diabetic retinopathy is achieved with the assistance of different deep learning and machine learning methods. This section reviews a few methods.

Ambaji S. Jadhav *et al.* [11] introduced robotized D.R. identification through retinal irregular identification thoughts, hemorrhages, Microaneurysms, and indelicate exudates. The ba and sic manipulation periods to the presented T.R. detection structure are pre-manipulation, optic disc discharge, vascular drainage, segmentation of abnormalities, feature extraction, optimal component selection, and classification classification. The retina image is now pre-manipulated with Contrast Limited Adaptive Histogram Equalization. Additionally, the following stage reveals the optic plate discharge, which can be done through the open-close hydraulic transition. Also, the gray level

threshold distorted, splitting the veins and expelling them. When the optic nerve and veins are removed, the division of the appendages is completed by a change of the upper cap and a capillary sieve.

Furthermore, the element extraction stage was initiated, which typically concentrated four systems of elements such as the local binary pattern, the textured energy computation, the Shannons, and the Kapur's entropy. Meanwhile, the distance of the element vector is the length of all accounts, and the process of determining the elements is done, which selects the extraordinary highlights with the slightest connection. In addition, the Deep Belief Network (DBN)-based arrangement calculation runs the sequence of images into four classifications of normal, pre-, moderate, or extreme levels. Better element selection is accomplished with an enhanced meta-heuristic calculation called Modified Gear in addition to the Steering-based Rider Optimization Algorithm (MGS-ROA); a similar calculation informs the load on the DBN.

Kamrul Hasan *et al.* [12] have introduced an end-to-end encoder-decoder network called DRNet for separating and controlling O.D. in addition to Fovea focus. In our DRNet, a Skip Association was proposed to compensate for lost spatial data by pooling it in the encoder, called the Residual Skip Association. Unlike the previous Skip Association in UNet, the Skip Association does not link low-level element maps directly from previous starting point layers with a decoder of a similar size. Here, authorize DRNet to use a variety of freely accessible databases such as IDRiD, RIMONE, DRISHTI-GS in addition to DRIVE aimed at the O.D. segment; IDRiD in addition to HRF aimed at O.D. focus control; And IDRiD aimed at the Fovea focus range.

Abubakar M. Ashir *et al.* [13] have introduced another method for retinal detection of diabetes from images. The proposed approach uses the element removed from the fundus image and the adjacent intensity data with the size of the heraldic highlights. The measured components encode Haralick features and use multi-solution data for various manifestations of diabetic retinopathy. The Long Short-Term Memory Network and the nearby Extrema Design provide a probable way to interrogate each part of the image with greater accuracy that assists in suppressing pseudo-positive events. This technique explores retinal vascularization in addition to hard-exudate manifestations of diabetic retinopathy in two various general data sets.

Cheng Wan *et al.* [14] have introduced a clever segmentation technique for various injuries in DR. This strategy is related to an active neural system and can be separated into encoder design, review design, and decoder design, so mentioned as EAD-Net. Afterward, standardization, in addition to expansion, the fundus images were sent from EAD-Net aimed at computerized highlight extraction and pixel-wise mark expectation. Assuming the rating of compatibility between recognized competitors and land actual lesions, our strategy is 92.77% response, 99.98% explicit, and 99.97% accuracy in the e_ophtha_EX database and AUPR IDRiD database under AUPR. In addition, the results of the nearby database show that our EAD-Net prefers performance over multiple scales, especially with a 10% improvement over the unique U-net.

Farzan Shenavarmasouleh *et al.* [15] have introduced convolutional neural networks (CNNs) in addition to transmission training to identify and develop the best segment for each event of injury seen in patients' fundus images. Here, creates a standardized information base from e-aphtha EX and e-ophtha M.A. and replaces the MaskMask R-CNN to identify minor lesions. Also, the information boost and pre-made loads of ResNet101 will compensate for the small amount of data. This model performs an auspicious test mAP of 0.45, showing that it can help physicians, in addition to ophthalmologists, spend time diagnosing. In treating, the popular D.R.

3. Proposed System Model

The proposed methodology contains five stages: dataset collection, preprocessing, segmentation, feature extraction and Classification, and parameter optimization. In the dataset collection stage, the retinal images are collected from normal and diabetic retinopathy patients. The collected data was filtered and standardized in the preprocessing stage. The region of interest was captured from the preprocessed images in the segmentation stage. In the fourth stage, feature extraction and Classification are performed using DCNN. Finally, the hyperparameters, such as weights, bias, batch size, filter size, etc., are fine-tuned using HBA in the optimization stage. The proposed process of the diabetic retinopathy detection method is presented in Figure 1. A detailed clarification of the projected methodology can be presented in the following section.

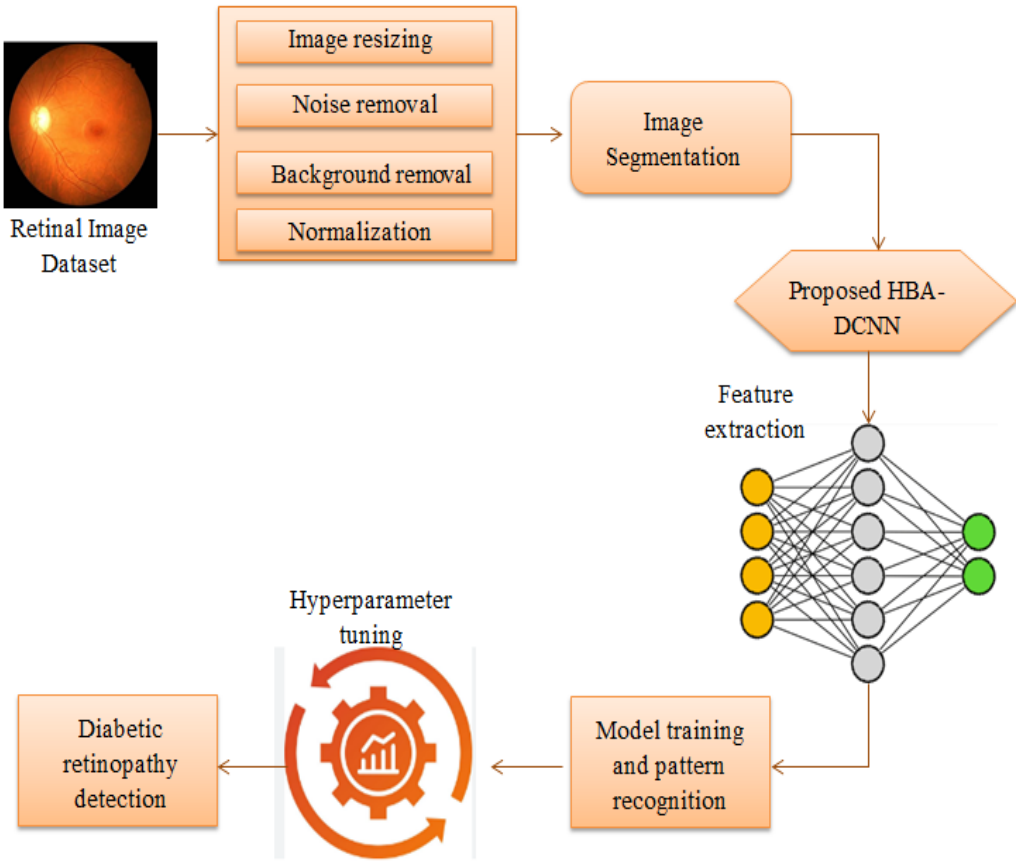

Figure 1: Architecture of the proposed methodology

3.1. Dataset collection

The proposed work begins with collecting retinal images from individuals affected by normal and diabetic retinopathy. Clinical experts label the collected images to indicate the presence of diabetic retinopathy. The presented study used two publicly available databases: DRIVE [16] and STARE [17]. These databases are available on the Kaggle site. The STARE database comprises 362 retinal images, and the dataset is 504.39 megabytes (M.B.). The STARE is a project initiated by Michael Goldbaum, M.D., at the University of California, San Diego, in 1975. Images and clinical data were offered by the Shiley Eye Center at the University of California, San Diego. Research scholars extensively use this database to develop classification or prediction algorithms.

On the other hand, the DRIVE database was obtained from a retinopathy screening program in The Netherlands. This database contains 40 retinal images, and their MaskMask was collected from 400 individuals between 25 and 90 years of age. The size of this database is 29 M.B., and the photos are captured using a Canon CR5 non-mydriatic 3CCD camera. These databases undergo preprocessing steps to remove the noise and other unwanted attributes. Figure 2 presents the sample's retinal images.

Figure 2: Dataset images

3.2. Preprocessing

Preprocessing is one of the crucial steps in diabetic retinopathy analysis. The image preprocessing includes image resizing, noise removal, background elimination, and normalization. In the image resizing step, the size of all images is standardized to ensure uniformity across the database. In the presented work, nearest neighbor interpolation was applied to resize all images, and they were resized into fixed dimensions of 512 x 512 pixels. The collected images are indeed affected by unnecessary artifacts, which reduce the segmentation and detection efficiency. The unnecessary artifacts should be removed from the pictures using the filtering technique. The median filter is used to remove the noises and to smoothen the image.

Median filtering

The median filter is a non-linear digital filtering approach employed in image processing applications to eliminate the noise from the images. This filtering mechanism efficiently preserves the edge while discarding noises. The median filter can smooth the fundus images. In addition, it gathers the complete particulars of the smoothened images. The median value is the median parameter of the complete neighbored pixel parameters [18]. The median parameter is more robust and considered the central parameter. The middle parameter is computed based on the below equation,

$$Median\ [A(X) + B(X) \neq Median[A(X)\} + Median\{B[X] \qquad (1)$$

Where($A.X$)and $B(X)$ can be considered as the different retinal images. The value of a pixel is replaced by a median of the intensity levels in the neighborhood of that pixel by the Median Filter. The preprocessed images are illustrated in Figure 3.

Figure 3: (a) Input and preprocessed image

Gabor filtering

Gabor filtering was employed to eliminate the background from the filtered retinal images. This filter efficiently identifies and emphasizes specific attributes in the images while suppressing irrelevant background information. This filter is utilized to enhance the small vessels of the fundus images. In the 2D images, the convolution is applied to Gabor filters where changing kernels were described as Gaussian ones changed by a sinusoid [19]. These

kernels are described as the Cartesian basis center, related to abscissa with orientation parameters. The sinusoid and Gaussian parameters of the Gabor filter are formulated as follows,

$$k_{\theta,\sigma,\gamma,\lambda,\varphi}(X,Y) = Exp\left(-\frac{x^2+\gamma^2y^2}{2\sigma^2}\right)COS\left(2\pi\frac{x}{\lambda}+\varphi\right) \quad (2)$$

where θ can be defined as Gabor's kernel function, φ can be described as phase offset, λ can be described as spatial wavelength, γ can be described as the ellipticity of the circular Gaussian and the sinusoid, σ can be described as the deviation. The pixel value is defined by the size of pixels (V_x,) Vy, and the center of the kernel, which has the translation function($s\ Ic\ and\ J_c$).

$$k_{\theta,\sigma,\gamma,\lambda,\varphi}(I,J) = Exp\left(-\frac{x^2+\gamma^2y^2}{2\sigma^2}\right)COS\left(2\pi\frac{X`}{\lambda}+\varphi\right) \quad (3)$$

Where,

$$X` = (I-I_c)V_x cos\theta + (J-J_c)V_x sin\theta$$
$$Y` = (I-I_c)V_x sin\theta + (J-J_c)V_x cos\theta \quad (4)$$

A Gabor kernel is designed with a parallel stripe with various weights, and it contains an ellipsoidal envelope with the kernel variables for managing the position of the stripes, orientation, and size. In the Gabor filtering, the image background is calculated and deleted by subtracting the filtered images from the median filtered images, considering a large kernel to empower the vessel structure by utilizing a circular structuring parameter with a radius of 8 pixels.

Z-score normalization

Finally, z-score normalization was applied to standardize the pixel intensity values of the retinal images. This step helps ensure consistent scale, which is crucial for enhancing the deep learning model's performance. The z-score value is determined for each pixel using Eqn. (5).

$$z-score = \frac{a-mn}{sta_{dv}} \quad (5)$$

Where a indicates the original pixel intensity value, mn defines the mean pixel intensity value, and sta_{dv} represents the standard deviation. After computing the z-score value, each pixel value is replaced with its z-score value. These preprocessing steps improve the image quality, reduce the computational complexity, and enhance the classification performance. In addition to these steps, data augmentation steps, such as rotating, flipping, zooming, etc., are performed to increase the number of image samples, which helps reduce overfitting challenges and improves the model's generalization efficiency.

3.3. Segmentation

To segment the blood vessels from the images, the superpixel mean orientation is utilized in the proposed methodology, which collects the superpixels by over-segmenting the image by considering a sensible conventional segmentation algorithm. Superpixel collects the multi-scale diversity in addition to the visual designs of traditional photos. The efficient combination of the signals from a higher multitude of superpixels presented an efficient outcome; Moreover, the superpixel segmentation with mean orientation can be utilized to improve the segmentation accuracy. The bipartite graph partitioning and superpixels are collected using the segmentation approach. The retinal image pixel with a minor constant parameter is considered in the bipartite graph partitioning. Additionally, it can be deleted to contrast the gathered superpixels.

Input: Input image and number of segments

Output: K-way segmentation of *I*

Step 1: Gathering a super pixel from the input image

Step 2: Develop a bipartite graph G {X: Y: B] with X=1US, Y=S in addition B is developed

Step 3: To compute k groups, the T-cut technique is applied.

Step 4: The pixels are considered to segment the same group in images

The input image is segmented using the mean orientation technique to extract the correct portion from the retinal image. In this method, mean shift gives additional deep data of objects and connects the portions considered to return gross segmentation. In this technique, mean shift is viewed as a clustering method. A comprehensive kernel technique is applied to compute nonparametric density [20]. Mean shift operation is defined as the window for each information point. In addition, it calculates the mean of data points. Change the window to the mean and repeat the method when it converges. The mean shift operation is utilized to achieve image segmentation, space analysis, mode seeking, clustering, and visual tracking. The kernel density can be considered an efficient computation technique in the proposed segmentation approach.

Presented N data points $I = 1,2,..,N$ with the D dimensional space, symmetric positive bandwidth matrix H, multivariable density estimator. At last, point X is calculated based on the below equation,

$$F(X) = \frac{1}{N}\sum_{I-1}^{N} K_H(X - X_I) \qquad (6)$$

Where,

$$K_H(X) = |H|^{-1/2} K\left(H^{-1/2}X\right) \qquad (7)$$

The multivariate kernel can be created from a symmetric univariate kernel K1(X) in twofold various ways, which are presented as follows,

$$K^P(X) = \prod_{I=1}^{D} K_1(X_I) K^S(X) = A_{K,D} K_1(X) \qquad (8)$$

Where $K^P(X)$ can be described as the univariate kernel product, $K^S(X)$ can be defined as the symmetric parameters. In this section, the radial symmetric kernels can be selected. A specific class of outwardly symmetric kernels can be compensated with the help of the below equation,

$$K(X) = C_{K,d} K(X^2) \qquad (9)$$

$(K.X)$ can be described as a constant parameter of 1 and is considered positive, $C_{.K.,d}$ can be described as normalization constant, $(and\ K.X)$ defines the kernel profile. The Euclidean metric rationality aimed at the feature space should be concluded. The single bandwidth variable is considered, and after that, it is formulated as follows,

$$F(X) = \frac{1}{NH_D}\sum_{I-1}^{N} K\left(\frac{X - X_I}{H}\right) \qquad (10)$$

Based on the mean square error, the kernel density estimator is computed. Based on the profile notation, the density estimator is formulated as follows,

$$F(X) = \frac{C_{K,d}}{NH_D}\sum_{I-1}^{N} K\left(\frac{X - X_I{}^2}{H}\right) \qquad (11)$$

Firstly, the original density with feature space F(X) can be computed using density models. The modes can be placed among the gradients. In addition, the mean shift procedure computes zeros deprived of computing the density function. The density gradient computation can be achieved as the density gradient estimator with the consideration of the linearity function. The blood vessel segmentation images are utilized to extract the feature vectors. Figure 3 presents the segmentation images.

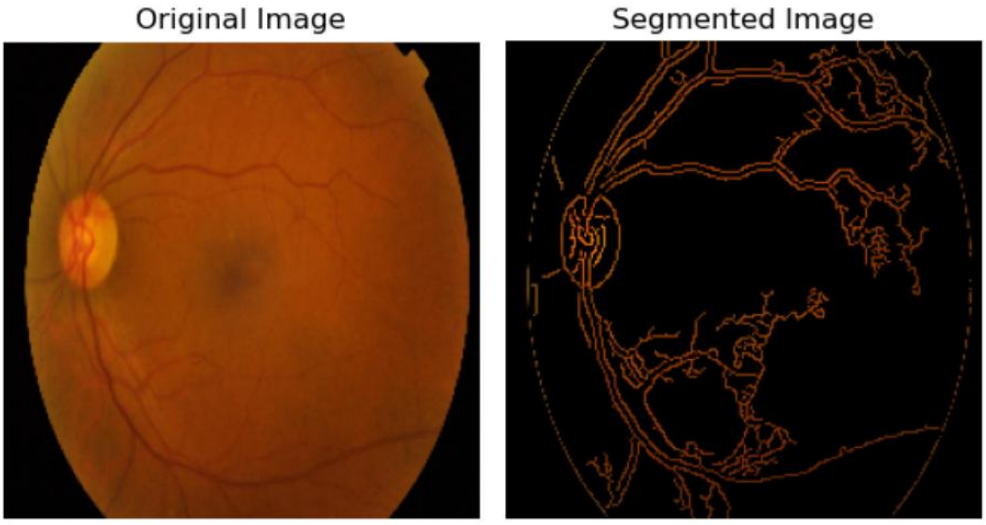

Figure 3: Segmented images

3.4. Feature Extraction and Classification

A DCNN is a type of artificial neural network, which has the efficiency of recognizing the patterns by analyzing the images. In recent decades, the DCNN was used in numerous computer-vision applications such as object detection, disease prediction, etc. In the proposed work, the DCNN was employed for identifying the presence of diabetic retinopathy by analyzing the retinal images. The architecture of DCNN is similar to CNN with additional convolutional and pooling layers. The general architecture of DCNN includes input layer, convolutional layers, pooling layers, fully connected layer and output layer. The input layer accepts the segmented images as input and transforms the image into an appropriate format to perform feature extraction and classification. The deep convolutional connections enable the system to learn hierarchical representations within the data, providing accurate classifications. The convolutional layer uses kernel filters and captures the local patterns and correlations within the segmented images. As a result, it produces feature maps highlighting the spatial interconnections and patterns in the input data. These features are essential in training the model for making accurate classification. The structure of the projected DCNN is presented in figure 4. The number of convolutional layer depends on the complexity of the problem and it is always associated with the activation function and pooling layer.

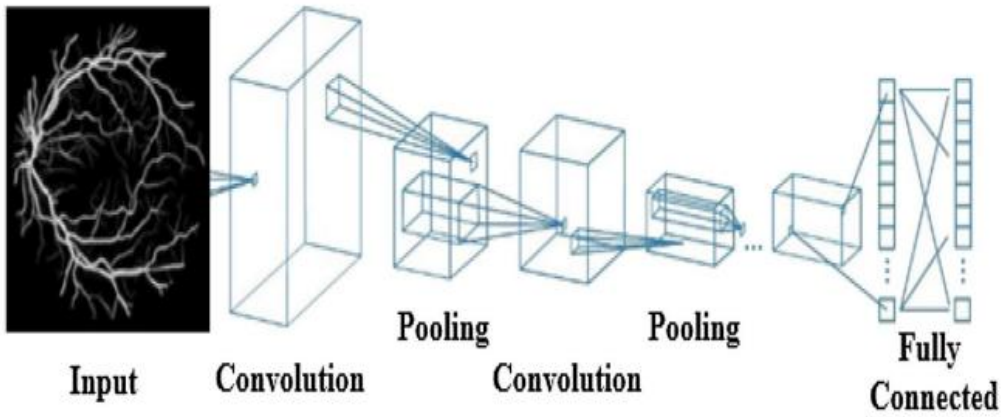

Figure 4: DCNN architecture

Convolutional layer

The convolutional layer is the core component of CNN. This layer accepts the formatted segmented retinal image from the input layer and applies a filter to extract the feature map. The filter is also known as a feature detector, which moves across the receptive image fields to identify the presence of a feature. This process is termed as convolution. In the proposed work, a kernel filter was applied with a size of 3x3. The feature map is performing dot products between the input pixels and the filter. The convolutional layer is formulated as below.

$$C_n = L_n * Is + B_n \quad (12)$$

Where C_n is the resultant of the n^{th} convolutional layers, L_n is the set of learnable parameters such as weight, Is defines the segmented image, and B_n denotes the bias term of the n^{th} convolutional layer. The learnable parameters (filters) are adjusted in the training phase through backpropagation. Following the convolutional layer, an activation function named Rectified Linear Unit (ReLU) was applied to introduce non-linearity. This activation function enables the DCNN to learn diverse features and spatial characteristics in the images.

Pooling layer

The extracted feature sequence from the convolutional layer is passed into the pooling layer. The pooling layer is also known as downsampling and it helps in reducing the dimension of the feature map, while preserving the most significant attributes. Similar to the convolutional operation, the pooling operation sweeps a filter across the input image. The major difference between these layers is the pooling filter does not have weights. Typically, there are two types of pooling namely: max pooling and average pooling. In the developed work, max pooling was used. In max pooling, the filter selects the pixel with the maximum value while moving across the input. After several convolutions and pooling operations, the final feature map is fed into the fully connected layer. This feature map contains all important attributes differentiating the normal and infected images. In addition, the extracted feature maps are flattened into a one-dimensional vector after the convolution and pooling layers for performing classification.

Fully connected layer

Fully Connected Layers take the feature map from the previous layer and computes the final classification. This layer performs the task of classification based on the features extracted through the previous layers and their different filters. The FC layers use a softmax activation function to classify inputs appropriately, producing a probability from 0 to 1, which is formulated below.

$$P_s = soft\max\left(W_o * F_c\right) + B_o \quad (13)$$

Where P_s is the probability value of classes (If it is greater than 0.5, the model predicts the class as normal, while the probability value is less than or equal to 0.5 then the model classifies the image as diabetic retinopathy infected image), $soft\max$ defines the activation function, W_o indicates the weight of the FC layer, and B_o refers to the FC layer bias vector. Although the DCNN offers improved results, its performance depends on the accurate selection of hyperparameter values. To optimally determine the hyperparameter values of DCNN, the HBA was used in the proposed work.

3.4.2. Honey badger algorithm (HBA)

The HBA is a meta-heuristic optimization algorithm developed based on the intelligent foraging characteristics of honey badger. The major advantage of the HBA is its effective search strategy for solving optimizing problems. In addition, the honey badger exhibits dynamic search behavior with digging and the honey finding techniques are formulated into exploitation and exploration phases. Also, this algorithm maintains sufficient population diversity even towards the end of the search process. In the proposed work, the HBA was employed for optimizing or finding the optimal values of the hyperparameters of DCNN. The main objective of the HBA is to reduce the error rate or loss incurred by the DCNN model while training. The candidate solution in HBA indicates the hyperparameter sequence and its position defines the hyperparameter value. The HBA is normally divided into two stages, the digging stage and the honey stage, which are presented in this portion. The mathematical preparation of

the HBA can be presented in this section. Additionally, the HBA proceeds with the exploitation and exploration stage and is considered a global optimization algorithm.

Step 1: Initialization phase

The initialization of the candidate solution can be formulated in the below equation,

$$Initial\ Population = \left[X_{11}\ X_{12}\ X_{13}\ \ldots\ X_{1D}\ X_{21}\ X_{22}\ X_{23}\ \ldots\ X_{2,D}\ \ldots\ \ldots\ \ldots\ \ldots\ \ldots\ X_{N1}\ X_{N2}\ X_{N3}\ \ldots\ X_{N,D}\ \right] \quad (14)$$

$$honey\ badger\ i^{th}\ position, X_I = [X_I^1, X_I^2, \ldots, X_I^D] \quad (15)$$

The initialization of the honey badges and the positions are formulated as follows,

$$X_I = LB_I + R_1 \times (UB_I - LB_I) \quad (16)$$

R_1 can be described as the random number between 0 and 1, UB_I can be described as the upper bound, LB_I can be defined as the lower bound, and X_I can be described as the honey badger position.

Step 2: Defining intensity phase

The intensity function is connected with the prey's concentration strength and distance. This formulation is presented below,

$$I_i = R_2 \times \frac{s}{4\pi D_i^2}, R_2 \quad (17)$$

$$s = (X_i - X_{i+1})^2 \quad (18)$$

$$D_i = X_{prey} - X_i \quad (19)$$

D_i can be described as the distance function of prey, s as source or concentration strength, and R_2 as a random number between 0 and 1.

Step 3: Update density factor

The density factor controls time-changing generalization to empower smooth conversion from exploitation to exploration. To update the process of decreasing factor, which diminishes with iteration functions to reduce the time randomization based on the below equation,

$$\alpha = c * exp\left(\frac{-t}{t_{max}}\right) \quad (20)$$

Where t_{max} can be described as a maximum number of iterations and c can be described as a constant parameter.

Step 4: Local optimum escaping scenario

This step optimizes local conditions in a specified region. In this step, the algorithm uses flag F to change the search method, aiming to consume many suggestions for the search agent to find the optimal space.

Step 5: Updating process

In the HBA algorithm, the position is updated by considering two sections: the honey stage and the digging stage.

Digging stage:

$$X_{new} = X_{prey} + F \times \beta \times I \times X_{prey} + F \times R_3 \times \alpha \times D_I \times |cos(2\pi R_4) \times [1 - cos(2\pi R_5)| \quad (21)$$

Here, F can be described as a flag that changes the search direction; D_I can be defined as the distance among prey; $R4\ and\ R_5$ can be described as random numbers between 0 and 1; β can be described as a random number with random numbers.

$$F = \{1\ if\ R_6 \leq 0.5\ -1\ else \quad (22)$$

R_6 can be described as a haphazard variable between 0 and 1; in the digging stage, the honey badger is sincerely presented in the small intensity function, denoted as I and X_{prey} can be described as the distance between badger and prey.

Algorithm 1: Pseudocode of the proposed methodology
Initialization of population "(present stride parameter of CNN)
Compute fitness function
Store optimal position and assign fitness function
While$T \leq T_{MAX}$**do**
Decreasing factor updating
For I=1 to N **do**
Compute the intensity values
If R<0.5 then
Update the position-based exploration
Else
Update the position-based exploitation
End if
Compute new position
End for
end while stop condition satisfied
save the optimal parameter
Return

Honey phase:

In this case, the honey badger shadows the honey leader bird towards the spread apiary, which is formulated as follows,

$$X_{new} = X_{prey} + F \times \beta \times R_7 \times D_I \qquad (20)$$

where X_{new} can be described as the new position. The proposed algorithm is usually related to global optimization because of the exploitation and exploration stages. To achieve easy implementation and understanding purposes, the number of operators must be minimized or adjusted [21]. With the help of the proposed methodology, blood vessel segmentation is achieved, and diabetic retinopathy is classified. The performance of the projected technology is presented in the following section.

4. Outcome Evaluation

This performance evaluation section implemented the projected technique in Python with 1 T.B. hard disc, 8GB RAM, Intel i5 Processor, and 3.0GHz. To compute the evaluation of the projected technique, it is analyzed with performance metrics, contrasted with the conventional techniques such as DNN and SVM, respectively. The two kinds of databases that are considered to validate the projected technique evaluation are STARE and DRIVE. Performance metrics like specificity, accuracy, recall, and F-measure validate the projected technique performances. The parameter values of the proposed strategy are presented in Table 1.

Table 1: Simulation Variables

S.No	Description	Parameters	Activation Size	Activation Shaper
1	Fully connected	17,602	140	(14,1)

2	Pooling 2	0	400	(5,5,16)
3	Convolution 2	424	1600	(10,10,16)
4	Pooling 1	0	1800	(15,15,8)
5	Convolution 1	212	7200	(30,30,8)
6	Input	0	12,288	(64,64,3)

To authenticate the presentation of the projected methodology, presentation metrics are utilized, which are formulated as follows: performance parameter can be described as the normal evaluation of results and discussions that initiate required information related to the efficiency of the projected technique through considering presentation measures like accuracy, precision, and specificity in addition to F-measure.

4.1. STARE database

The proposed methodology is evaluated in each database using conventional methods such as DNN and SVM. Performance metrics, such as accuracy, precision, recall, and specificity, are utilized to validate the proposed methodology in addition to the F-measure.

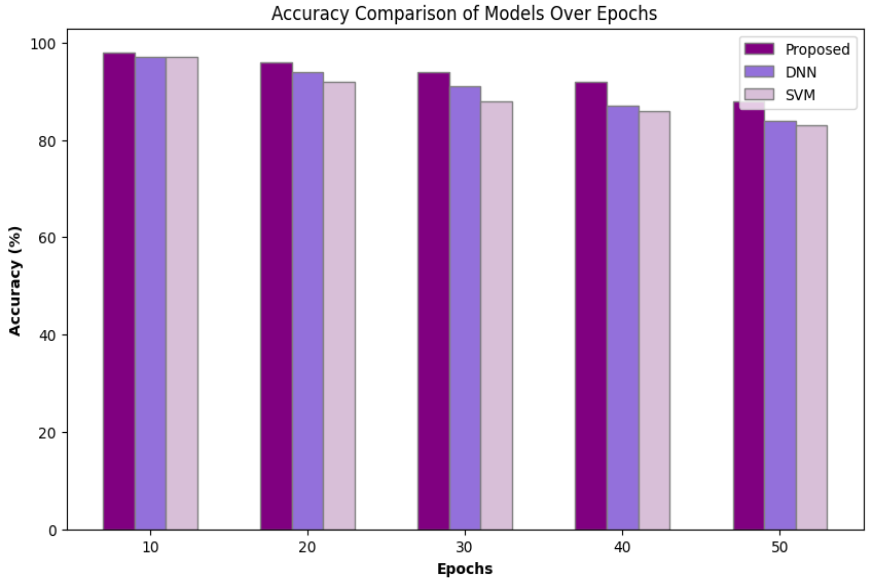

Figure 5: Accuracy measurement

The accuracy measure of the projected methodology is presented in Figure 5. The proposed technique achieved 99% accuracy in epoch 10. Similarly, for varying epochs like 20, 30, 40, and 50, the proposed methodology obtained accuracy of 93%, 92%, 88%, and 86%, respectively. The DNN method achieved 90% of accuracy in epoch 10. Similarly, the DNN model earned 88%, 85%, 83%, and 82% of accuracy in the diabetic retinopathy detection for different epochs such as 20, 30, 40, and 50, while the SVM method achieved 82% accuracy in epoch 10 and 83%, 84%, 82%, and 80% of accuracy for varying epochs such as 20, 30, 40, and 50. This illustrates that the developed algorithm achieved better accuracy than others.

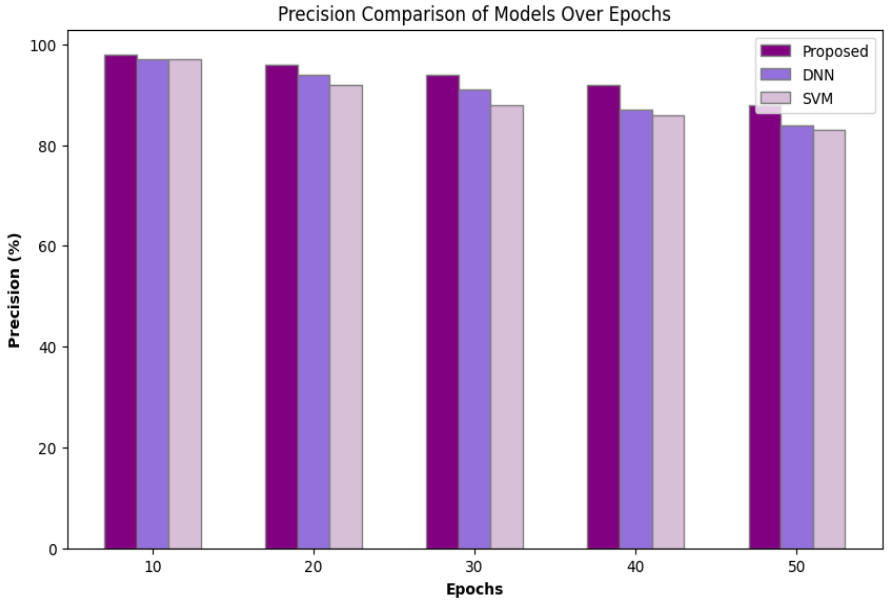

Figure 6: Precision measurement

The precision measure of the projected technique is presented in Figure 6. The proposed method achieved precision of 99.9%, 95%, 93%, 89%, and 83% for varying epoch counts such as 10, 20, 30, 40, and 50, respectively, while the conventional DNN model obtained 88%, 85%, 83%, 81%, and 80% of precision for different epochs such as 10, 20, 30, 40, and 50. The SVM method achieved 78%, 78%, 75%, 72%, and 70% of precision in the diabetic retinopathy detection for varying epochs such as 10, 20, 30, 40, and 50. From this assessment, it is evident that the proposed strategy earned improved precision compared to other techniques like DNN and SVM, which demonstrates its reliability and effectiveness in providing more accurate detection and classification of diabetic retinopathy.

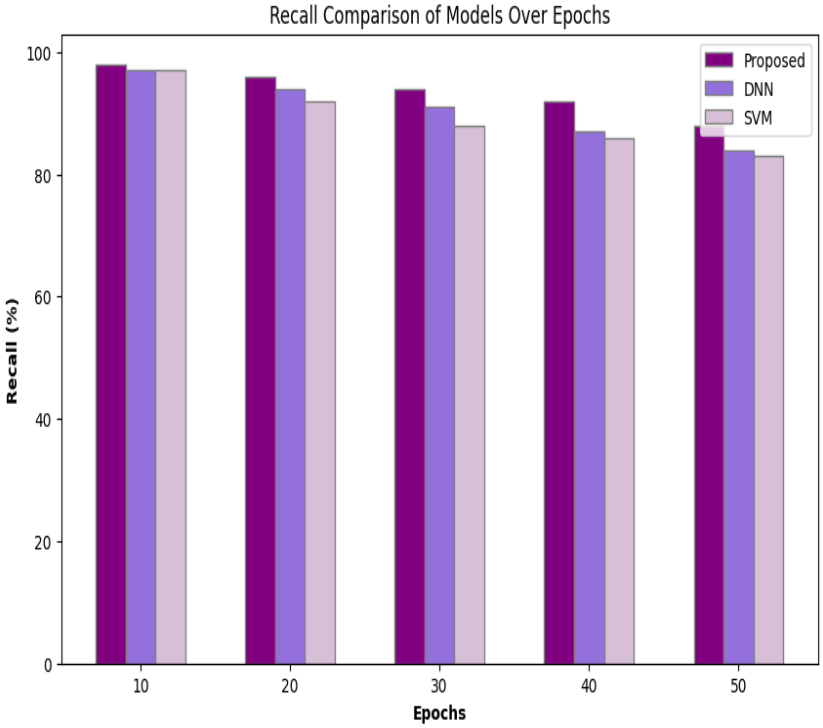

Figure 7: Recall measurement

The recall measure of the projected methodology is presented in Figure 7. The proposed technique achieved 97% recall in epoch 10. Similarly, the designed strategy obtained 91%, 89%, 85%, and 82% of recall in the diabetic retinopathy detection for different epochs such as 20, 30, 40, and 50. On the other hand, the DNN method achieved 87% of recall in epoch 10 and 85%, 83%, 80%, and 82% of recall in the diabetic retinopathy detection for different epochs such as 20, 30, 40, and 50. Similarly, the SVM method achieved 80% recall for epoch 10 and 78%, 75%, 72%, and 70% of recall in the diabetic retinopathy detection for different epochs such as 20, 30, 40, and 50. This analysis illustrates that compared to the existing models the proposed algorithm achieved better recall, highlighting its potential in identifying the most stringent attributes for precise classification and detection of diabetic retinopathy.

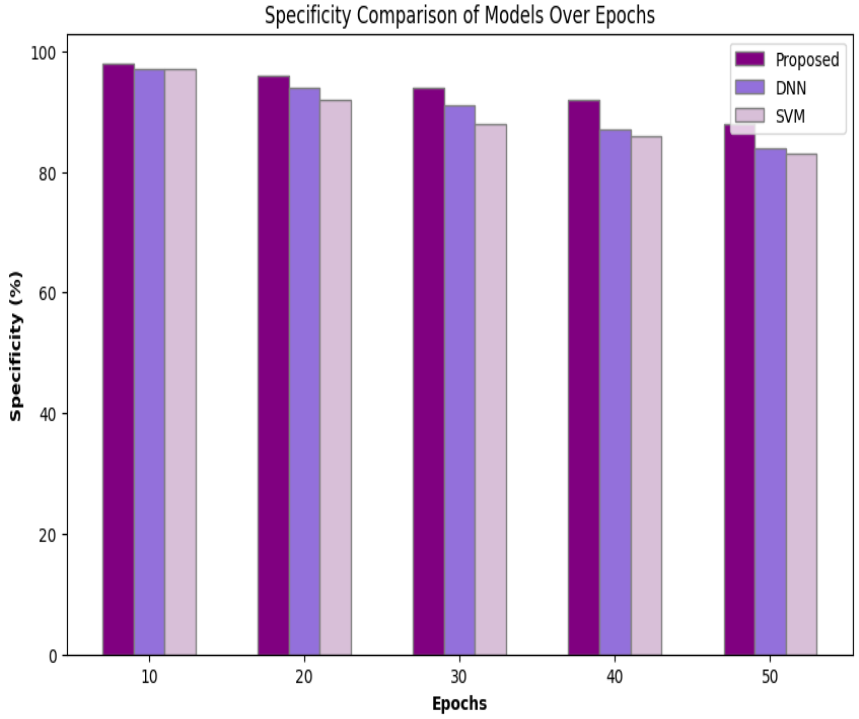

Figure 8: specificity measurement

The specificity measure of the projected technique is presented in Figure 8. On implementation, it is observed that the proposed framework achieved 95%, 90%, 87%, 85%, and 83% of specificity in the non-diabetic retinopathy detection for different epochs such as 10, 20, 30, 40, and 50. But the existing DNN method obtained comparatively lower specificity of 85%, 80%, 78%, 80%, and 81% in the non-diabetic retinopathy detection for different epochs such as 10, 20, 30, 40, and 50. Similarly, the SVM methodology attained 81%, 81%, 78%, 75%, and 72% of specificity in the non-diabetic retinopathy detection for different epochs such as 10, 20, 30, 40, and 50. The enhancement of specificity demonstrates that the presented methodology categorizes the non-diabetic retinopathy cases with greater accuracy.

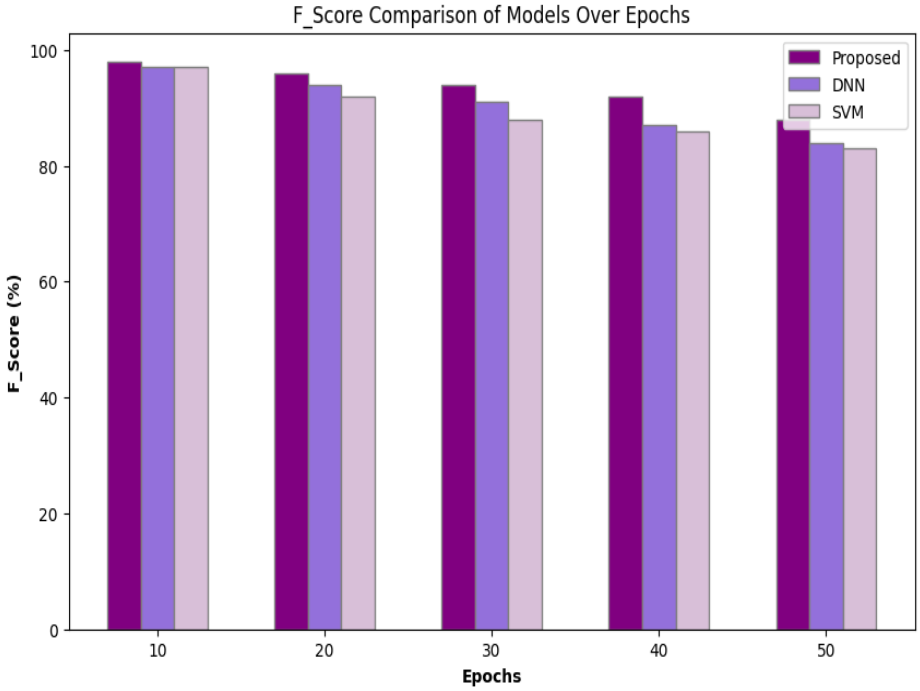

Figure 9: F-measure measurement

The F-measure measure of the projected methodology is presented in Figure 9. The conventional strategies used for comparative evaluation include DNN and SVM. The DNN method achieved 85%, 84%, 83%, 81%, and 80% of F-measure different epochs such as 10, 20, 30, 40, and 50, while the SVM approach earned F-measure of 80%, 78%, 75%, 72%, and 70% for different epochs such as 10, 20, 30, 40, and 50. But the proposed technique achieved relatively higher F-measure of 95%, 88%, 85%, 83%, and 80% of F-measure in the diabetic retinopathy detection for different epochs such as 20, 30, 40, and 50. The increased F-measure illustrates that the proposed algorithm offers greater balance between the classification of positive and negative classes.

4.2. DRIVE databases

In each database, the proposed methodology is evaluated using conventional methods such as DNN and SVM. Performance matrices validate the proposed methodology, such as accuracy, precision, recall, specificity, and F-measure.

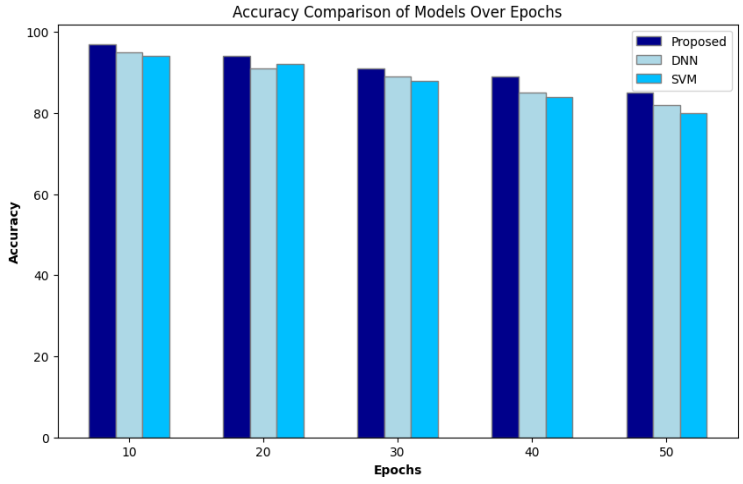

Figure 10: Accuracy measurement

The accuracy measure of the projected technique is illustrated in Figure 10. The proposed method achieved 99.9%, 96%, 95%, 92%, and 91% of accuracy in the diabetic retinopathy detection for different epochs such as 10, 20, 30, 40, and 50. On the other hand, the existing DNN model obtained 89%, 92%, 91%, 89%, and 84% accuracy in the diabetic retinopathy detection for different epochs such as 10, 20, 30, 40, and 50, respectively and the conventional SVM model incurred 85%, 83%, 81%, 80%, and 78% of accuracy in the diabetic retinopathy detection for different epochs such as 10, 20, 30, 40, and 50. The increased accuracy in the designed methodology over the existing algorithms highlights its proficiency in identifying and classifying the diabetic retinopathy cases.

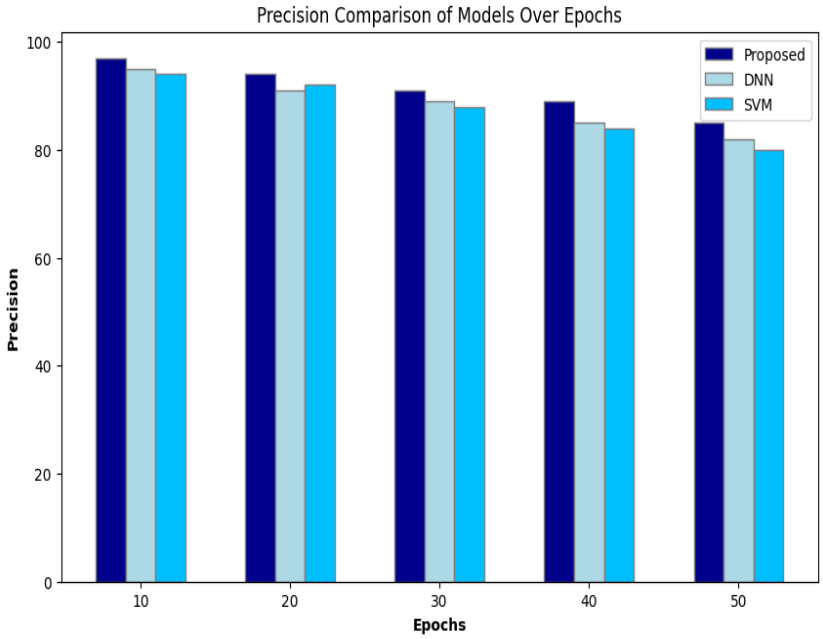

Figure 11: Precision measurement

The precision measure of the projected technique is presented in Figure 11. The SVM approach attained 82%, 78%, 74%, 75%, and 71% of precision in the diabetic retinopathy detection for different epochs such as 10, 20, 30, 40, and 50. On the other hand, the DNN methodology earned precision of 87%, 82%, 80%, 78%, and 75% for different epochs such as 10, 20, 30, 40, and 50. But the proposed framework achieved greater precision of 98.5%, 94.87%, 93.12%, 89%, and 85% for different epochs such as 10, 20, 30, 40, and 50. The improvement of precision demonstrates that the developed algorithm correctly categorizes the diabetic retinopathy instances from the eye retina images.

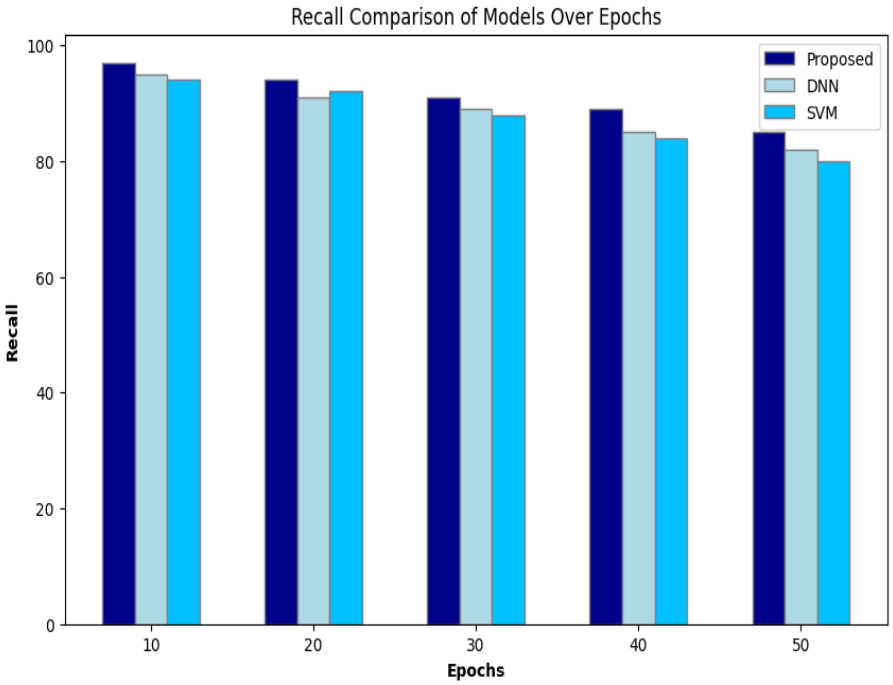

Figure 12: Recall measurement

The recall measure of the projected technique is presented in Figure 12. The DNN model achieved 87%, 84%, 82%, 81%, and 80% of recall in the diabetic retinopathy detection for different epochs such as 10, 20, 30, 40, and 50, while the SVM method earned 80%, 75%, 73%, 70%, and 68% of recall in the diabetic retinopathy detection for different epochs such as 10, 20, 30, 40, and 50. But the proposed method achieved comparatively higher recall rates of 95%, 90%, 87%, 84%, and 80% for different epochs such as 10, 20, 30, 40, and 50. This manifests that the designed framework effectively categorizes the retinopathy instances by understanding the linear interconnections within the input images.

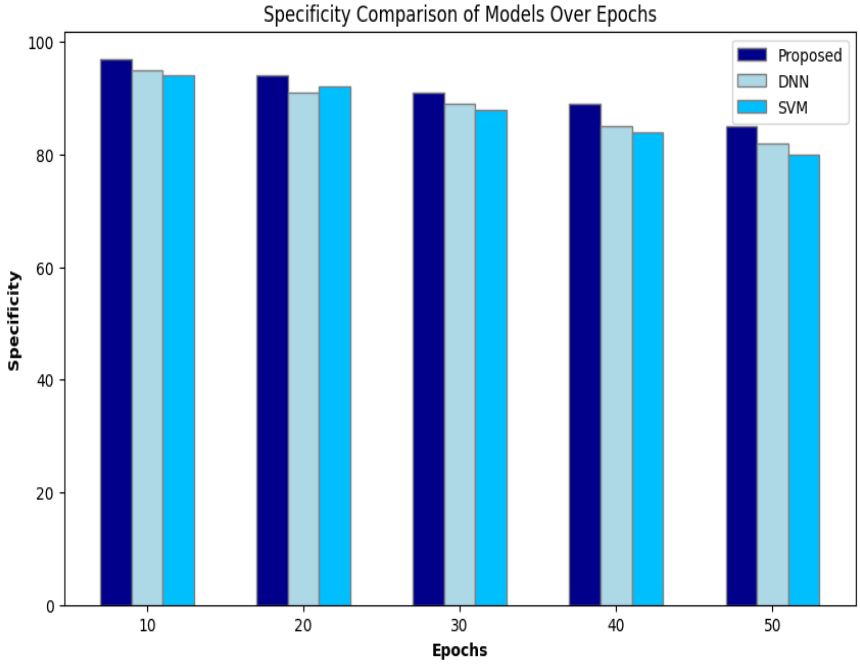

Figure 13: Specificity measurement

The specificity measure of the projected technique is presented in Figure 13. The presented method obtained 94%, 89%, 85%, 83%, and 80% of specificity in the diabetic retinopathy detection for different epochs such as 10, 20, 30, 40, and 50, respectively. But the existing DNN approach attained 86%, 82%, 80%, 75%, and 72% of specificity in the diabetic retinopathy detection for different epochs such as 10, 20, 30, 40, and 50. On the other hand, the SVM methodology earned 82%, 83%, 85%, 75%, and 70% of specificity in the diabetic retinopathy detection for different epochs such as 10, 20, 30, 40, and 50. This highlights that the developed algorithm precisely classifies the retinopathy and non-retinopathy instances.

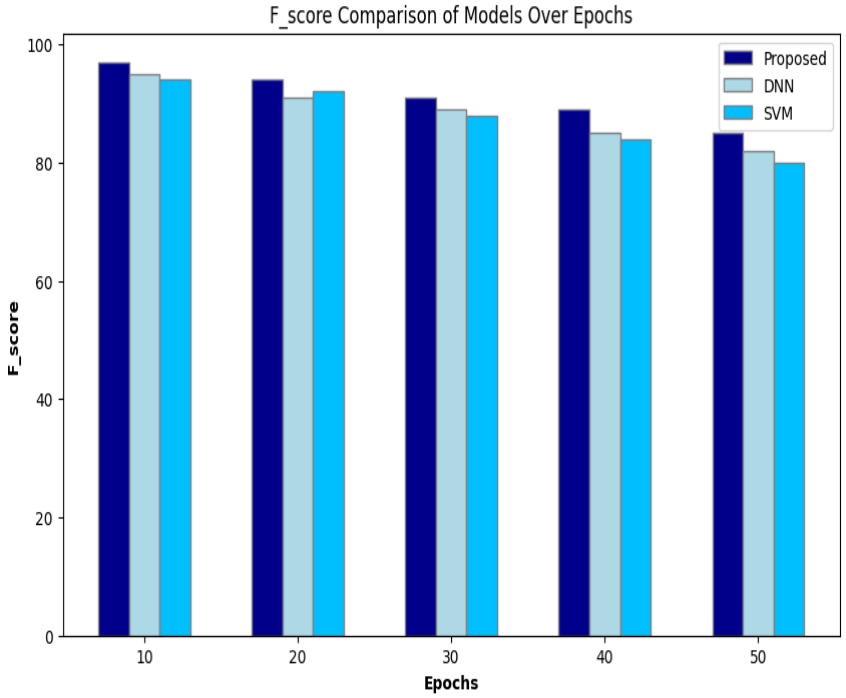

Figure 14: F-measure measurement

The F-measure measure of the projected methodology is presented in Figure 14. The proposed method achieved 94% of the F-measure in epoch 10. Similarly, the proposed methodology earned 89%, 84%, 81%, and 78% of F-measure in the diabetic retinopathy detection for different epochs such as 20, 30, 40, and 50. The DNN method achieved 84%, 83%, 82%, 80%, and 79% of F-measure in the diabetic retinopathy detection for different epochs such as 10, 20, 30, 40, and 50, respectively, while the SVM method achieved 80%, 78%, 75%, 72%, and 70% of F-measure in the diabetic retinopathy detection for different epochs such as 10, 20, 30, 40, and 50. Based on the analysis, it is evident that the proposed technique has attained higher f-measure than the existing models.

4.3 Discussion

This study proposed an automatic diabetic retinopathy classification model leveraging the benefits and advantages of DCNN and HBA. The proposed strategy used two retinal image databases, DRIVE and STARE, for training and validation. The images collected from the datasets are preprocessed by following steps like image resizing, filtering, background removal, and normalization. Consequently, image segmentation was performed using superpixel mean orientation. The diabetic retinopathy classification was done using the proposed HBA-DCNN. The DCNN module processes the segmented images and extracts the most informative and essential features that differentiate the infected eye from the average.

On the other hand, the HBA continuously optimizes and refines the hyperparameters of the DCNN model, which boosts its training efficiency and reduces the error and loss rate. The presented framework was modeled and implemented in Python, and the results are determined in terms of accuracy, precision, recall, f-measure, and

specificity. Table 2 presents the comparative assessment of the average performance of the proposed strategy with the existing techniques. The comparative evaluation shows that the developed algorithm achieved better results than others. These improved performances make the presented strategy effective and reliable for clinical applications to detect the presence of diabetic retinopathy.

Table 2: Comparative assessment of model's performances with existing models

Metric	Proposed	DNN	SVM
Accuracy (%)	94.98	89	81.4
Precision (%)	92.7	82.4	76
Recall (%)	87.2	82.8	73.2
Specificity (%)	86.2	77	79
F-measure (%)	85.2	81.6	75

5. Conclusion

A hybrid classification model was developed in this study to accurately identify the presence of diabetic retinopathy by analyzing the retinal images. The novelty of the proposed methodology lies in the seamless integration of DCNN and HBA into a single approach for fast and reliable disease prediction. The proposed work followed general image processing steps like preprocessing and segmentation to enhance the model's interpretability and computational efficiency. The DCNN processes the segmented images and learns the pattern difference between the infected and normal eyes. At the same time, the HBA uses its optimization capability to explore the hyperparameter space and determine its optimal value. This innovative combination offers improved accuracy, increases training speed, and reduces computational complexity. The experimental results demonstrated that the designed strategy achieved an average of 94.98% accuracy, 92.7% precision, 87.2% recall, 86.2% specificity, and 85.2% f-measure. In addition, the comparative assessment with the existing models like DNN and SVM manifests that the proposed strategy earned improved results compared to others. Although the proposed strategy achieved improved accuracy, more than these performances are needed for real-time scenarios. Hence, future studies should focus on developing a multi-objective classification model for improving performance.

References

1. Sehrish Qummar, Fiaz Gul Khan, Sajid Shah, Ahmad Khan, Shahaboddin Shamshirband, Zia Ur Rehman, Iftikhar Ahmed Khan, and Waqas Jadoon. "A deep learning ensemble approach for diabetic retinopathy detection." IEEE Access 7,pp.150530-150539,2019.
2. Shaohua Wan, Yan Liang, and Yin Zhang. "Deep convolutional neural networks for diabetic retinopathy detection by image classification." *Computers & Electrical Engineering* 72, pp. 274-282,2018.
3. Ramon Pires, Sandra Avila, Jacques Wainer, Eduardo Valle, Michael D. Abramoff, and Anderson Rocha. "A data-driven approach to referable diabetic retinopathy detection." *Artificial intelligence in medicine* 96, pp.93-106,2019.
4. Hamid Safi, Sare Safi, Ali Hafezi-Moghadam, and Hamid Ahmadieh. "Early detection of diabetic retinopathy." Survey of Ophthalmology 63, no. 5, pp. 601-608,2018.
5. Borys Tymchenko, Philip Marchenko, and Dmitry Spodarets. "Deep learning approach to diabetic retinopathy detection." arXiv preprint arXiv:2003.02261 2020.
6. Zhe Wang, Yanxin Yin, Jianping Shi, Wei Fang, Hongsheng Li, and Xiaogang Wang. "Zoom-in-net: Deep mining lesions for diabetic retinopathy detection." *In International Conference on Medical Image Computing and Computer-Assisted Intervention*, pp. 267-275. Springer, Cham, 2017.

7. D.Jude Hemanth, Omer Deperlioglu, and Utku Kose. "An enhanced diabetic retinopathy detection and classification approach using deep convolutional neural network." *Neural Computing and Applications* 32, no. 3, pp.707-721,2020.
8. Lifeng Qiao, Ying Zhu, and Hui Zhou. "Diabetic retinopathy detection using a prognosis of microaneurysm and early diagnosis system for non-proliferative diabetic retinopathy based on deep learning algorithms." IEEE Access 8, pp.104292-104302,2020.
9. Gabriel Tozatto Zago, Rodrigo Varejão Andreão, Bernadette Dorizzi, and Evandro Ottoni Teatini Salles. "Diabetic retinopathy detection using red lesion localization and convolutional neural networks." *Computers in biology and medicine* 116, pp.103537,2020.
10. Xianglong Zeng, Haiquan Chen, Yuan Luo, and Wenbin Ye. "Automated diabetic retinopathy detection based on binocular siamese-like convolutional neural network." IEEE Access 7, pp.30744-30753,2019.
11. Ambaji S. Jadhav, Pushpa B. Patil, and Sunil Biradar. "Optimal feature selection-based diabetic retinopathy detection using improved rider optimization algorithm enabled with deep learning." Evolutionary Intelligence 14, no. 4, pp.1431-1448,2021.
12. Md Kamrul Hasan, Md Ashraful Alam, Md Toufick E. Elahi, Shidhartho Roy, and Robert Martí. "DRNet: Segmentation and localization of optic disc and Fovea from diabetic retinopathy image." *Artificial Intelligence in Medicine* 111, pp.102001,2021.
13. Abubakar M. Ashir, Salisu Ibrahim, Mohammed Abdulghani, Abdullahi Abdu Ibrahim, and Mohammed S. Anwar. "Diabetic Retinopathy Detection Using Local Extrema Quantized Haralick Features with Long Short-Term Memory Network." *International Journal of Biomedical Imaging* 2021.
14. Cheng Wan, Yingsi Chen, Han Li, Bo Zheng, Nan Chen, Weihua Yang, Chenghu Wang, and Yan Li. "EAD-net: a novel lesion segmentation method in diabetic retinopathy using neural networks." *Disease Markers* 2021.
15. Farzan Shenavarmasouleh, and Hamid R. Arabnia. "Drdr: Automatic masking of exudates and microaneurysms caused by diabetic retinopathy using mask r-cnn and transfer learning." *In Advances in Computer Vision and Computational Biology*, Springer, Cham, pp. 307-318. 2021.
16. The STARE dataset is accessible at https://www.kaggle.com/datasets/vidheeshnacode/stare-dataset?resource=download&select=im0003.ppm
17. The DRIVE dataset is accessible at https://www.kaggle.com/datasets/andrewmvd/drive-digital-retinal-images-for-vessel-extraction
18. T. Vijayan, M. Sangeetha, A. Kumaravel, and B. Karthik. "Gabor filter and machine learning based diabetic retinopathy analysis and detection." *Microprocessors and Microsystems*, pp.103353,2020.
19. Kishore Balasubramanian, and N. P. Ananthamoorthy. "Robust retinal blood vessel segmentation using convolutional neural network and support vector machine." *Journal of Ambient Intelligence and Humanized Computing* 12, no. 3, pp. 3559-3569,2021.
20. Maria V. Valueva, N. N. Nagornov, Pavel A. Lyakhov, Georgii V. Valuev, and Nikolay I. Chervyakov. "Application of the residue number system to reduce hardware costs of the convolutional neural network implementation." *Mathematics and Computers in Simulation* 177, pp.232-243,2021.